

Ballistic Impact Behavior of Thick Composites: Analytical Formulation

N. K. Naik* and A. V. Doshi†
Indian Institute of Technology Bombay, Mumbai 400 076, India

Structures undergo different loading conditions during their service life. Impact is one of the typical cases of loading. In this study, an analytical method is presented for the prediction of ballistic impact behavior of thick composites based on wave theory and energy balance between the projectile and the target. For thick composites the wave propagation along the thickness direction is also considered. During the ballistic impact event, energy transfer takes place from the projectile to the target. As the energy is absorbed by different mechanisms, kinetic energy and velocity of the projectile decrease. Different damage and energy-absorbing mechanisms for a typical woven fabric composite are compression of the target directly below the projectile, possible reverse bulge formation on the front face, compression in the surrounding region of the impacted zone, tension in the yarns, shear plugging, bulge formation on the back face, delamination and matrix cracking, friction between the target and the projectile, and heat generation caused by impact. Based on the analytical method presented, typical results are generated and compared with the experimental values.

Nomenclature

A	= cross-sectional area of the projectile
A_{ql}	= quasi-lemniscate area reduction factor
A_y	= cross-sectional area of the yarn
d	= diameter of the projectile
dc_i	= deceleration of the projectile during a given time interval
E	= energy
E_{bb}	= energy absorbed due to bulge formation on the back face of the target
E_{cf}	= energy absorbed due to compression of the target directly below the projectile
E_{csy}	= energy absorbed due to compression of yarns in the surrounding region of the impacted zone: region 2
E_{dl}	= energy absorbed due to delamination
E_{fr}	= energy absorbed due to friction
E_{hg}	= energy absorbed due to heat generated
E_{mc}	= energy absorbed due to matrix cracking
E_{mt}	= energy absorbed by matrix cracking per unit volume
E_{rb}	= energy absorbed due to reverse bulge formation on the front face of the target
E_{sp}	= energy absorbed due to shear plugging of the yarns
E_{tf}	= energy absorbed due to tension in the yarns in a layer
E_{TOTAL}	= total kinetic energy lost by the projectile
F	= total force/contact force
F_c	= compressive force
F_i	= inertial force
G_{IICd}	= critical strain energy release rate in mode II
h	= thickness of the target
h_l	= thickness of each layer
h_{lc}	= thickness of a layer after compression
h_p	= length of the plug
K	= numerical constant (depends on the shape of the projectile)

KE_p	= kinetic energy of the projectile at a particular time interval
KE_{p0}	= kinetic energy of the projectile: incident
l	= length of the projectile
m	= mass of the projectile
m_0	= initial mass of the projectile
n_{lfs}, n_s	= number of layers failed due to shear plugging
n_{lt}	= number of layers failed in tension
n_{lsc}	= number of layers strained in compression
P_d	= percent delaminating layers
P_m	= percent matrix cracking
r	= radius of the projectile
S_{sp}	= shear plugging strength
t	= time/contact duration
V	= incident impact velocity/velocity
V_{BL}	= ballistic limit velocity
V_f	= fiber volume fraction
V_i	= velocity of the projectile at the i th instant
V_{zl}	= velocity of compressive-stress wave in z direction
V_{zt}	= velocity of shear-stress wave in z direction
x_d	= distance up to which damage has reached
x_l	= distance the longitudinal wave has traveled in x direction
x_{ll}, r_p	= distance the longitudinal wave has traveled in x direction in a layer
x_{llc}	= change in length of the yarn after tension
x_t	= distance the transverse wave has traveled in x direction
x_{tl}, r_t	= distance the transverse wave has traveled in x direction in a layer
z	= total depth the projectile has penetrated/projectile displacement
z_i	= depth of projectile penetrated during a given time interval
z_l	= distance the compressive-stress wave has traveled in z direction
z_{pl}	= distance by which a layer has moved in forward direction from its original position
z_t	= distance the shear-stress wave has traveled in z direction
γ	= shear strain
Δh_{lc}	= thickness by which a layer is compressed
Δt	= increment in time interval
ε_{cz}	= compressive strain along the thickness direction
ε_{\max}	= ultimate strain
ε_t	= tensile strain along the radial direction

Received 4 July 2004; revision received 23 November 2004; accepted for publication 24 November 2004. Copyright © 2005 by the American Institute of Aeronautics and Astronautics, Inc. All rights reserved. Copies of this paper may be made for personal or internal use, on condition that the copier pay the \$10.00 per-copy fee to the Copyright Clearance Center, Inc., 222 Rosewood Drive, Danvers, MA 01923; include the code 0001-1452/05 \$10.00 in correspondence with the CCC.

*Professor, Aerospace Engineering Department, Powai; nknaik@aero.iitb.ac.in.

†Graduate Student, Aerospace Engineering Department, Powai.

ε_{txl}	tensile strain in x direction in a layer
ρ	density of the target material
σ_{cz}	compressive stress along the thickness direction
σ_{\max}	ultimate stress
σ_r	tensile stress along the radial direction
σ_{tx}	tensile stress along the radial direction
τ	shear stress

I. Introduction

COMPOSITE materials are increasingly used in primary components in aerospace, marine, and civil applications. They offer significant advantages over the traditional metals/alloys by virtue of their high specific stiffness and high specific strength. They are designed to achieve unique mechanical and thermal properties and superior performance characteristics.

As technologies of composites manufacturing are advancing and applications of composites to nonaerospace industries are increasing, more and more thick section composites are used in structural designs. Thick composites behave differently compared to thin composites under impact loading conditions.

Based on the phenomenon of energy transfer between the projectile and the target, energy dissipation and damage mechanisms, the impact phenomenon is classified into three categories: low-velocity impact, high-velocity impact, and hypervelocity impact. The reason for this classification is that energy transfer between projectile and target, energy dissipation, and damage mechanisms in the target undergo drastic changes as the velocity of the projectile changes. An impact event is considered to be a low-velocity impact if the contact duration of impact is longer than the time period of the lowest vibrational mode of the structure. On the other hand, in high velocity or ballistic impact the contact duration of impact is much smaller than the time period of the lowest vibrational mode of the structure. Hypervelocity impact involves projectiles moving at extremely high velocities such that the local target materials behave like fluids. Ballistic impact is an impact caused by a propelling source, generally of low mass and high velocity.

It is important to understand the energy dissipation and the damage mechanisms of composites. Available experimental studies in the literature are specific to certain types of materials under certain ballistic impact conditions.^{1–14} Based on these experimental studies, the ballistic impact behavior of a class of composite materials cannot be understood. For complete understanding of this phenomenon, analytical studies are needed. Few analytical studies are available in literature.^{9,15–24} But the analytical models presented are not complete, and they do not take into account all of the energy-absorbing and damage mechanisms. More analytical studies are needed based on all energy-absorption mechanisms. Considerable attention has been given to understand the ballistic impact on thin composites. Relatively less progress has been made in understanding the behavior of thick composites under ballistic impact.

II. Impact Loading on Bodies

When an impact load is applied to a body, the stresses are set in. But the stresses are not immediately transmitted to all parts of the body. The remote portions of the body remain undisturbed for sometime. The stresses progress in all directions through the body in the form of disturbances of different types. In other words, stresses (and its associated deformations or strains) travel through the body at specific velocities. These velocities are functions of the material properties. Regardless of the method of application of impact load, the disturbances generated have identical properties based only on the target material properties. The progressions of the stress disturbances are called waves.²⁵

During an impact event, different types of waves propagate in the bodies depending on how the motion of the particles of the body is related to the direction of propagation of the waves and the boundary conditions. A particle can be defined as a small discrete portion of the solid. The most common types of waves in bodies are given in Ref. 25.

III. Thick Composites Analysis

During an impact event, the stress wave propagation takes place in all of the directions. Generally, this problem is analyzed using one-, two-, or three-dimensional approaches. A one-dimensional approach is based on string analysis,^{24,26} whereas a two-dimensional approach is based on membrane analysis.²³ In such studies the wave propagation along through the thickness direction is not considered. When these approaches are used to analyze structures, isotropic as well as orthotropic, it is assumed that the deformation behavior along the thickness direction of the target is the same along the entire thickness. Such an assumption can be made for targets of lower thickness or, in other words, can be used for thin plates. If the thickness of the plate is increased, the deformation and the induced stress behavior of the plate would be different at different locations along the thickness direction. For such cases the analysis is based on also considering the wave propagation along the thickness direction.

IV. Different Energy-Absorbing Mechanisms

Different energy-absorbing mechanisms are compression of the target directly below the projectile, possible reverse bulge formation on the front face, compression in the surrounding region of the impacted zone, tension in the yarns, shear plugging, bulge formation on the back face, delamination and matrix cracking, friction between the target and projectile, and heat generation due to impact. Different materials respond differently because the dominant energy-absorbing mechanisms can be different for each case. Impacted materials can fail in a variety of ways. The actual mechanisms depend on such variables as projectile size, shape, mass and velocity, and target material properties and geometry and relative dimensions of the projectile and target. Figure 1 shows different damage and energy-absorbing mechanisms in thick composites during ballistic impact event. Although one of these can dominate the energy-absorbing process, it would frequently be accompanied by several

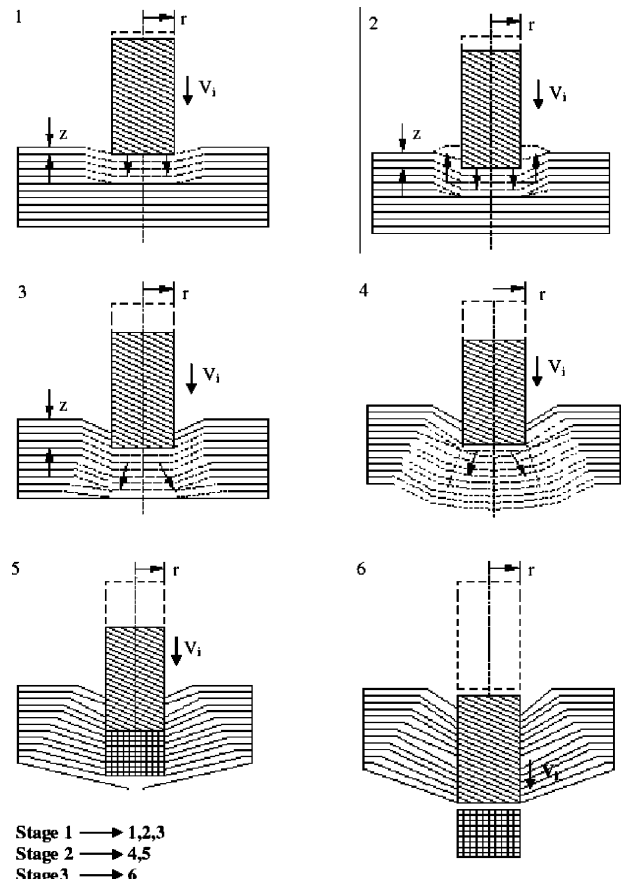


Fig. 1 Different damage mechanisms in thick composites during ballistic impact event.

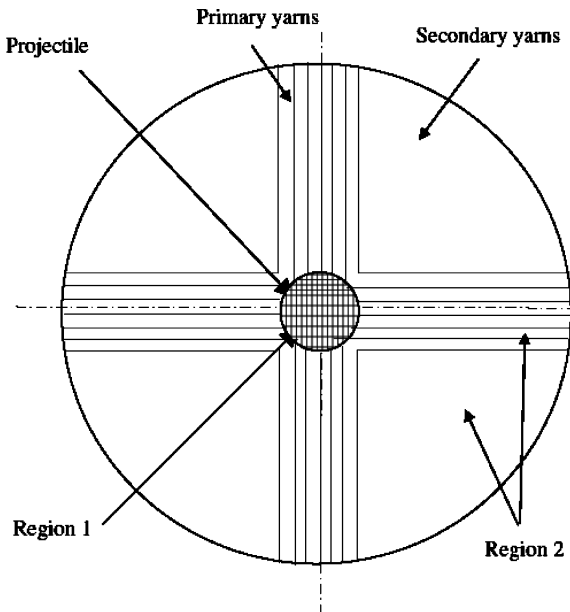


Fig. 2 Front view of a typical woven fabric thick composite target during ballistic impact event.

other modes. A front view of a typical woven fabric thick composite target is shown in Fig. 2. The yarns directly below the projectile are called primary yarns. These yarns provide the resistive force to the projectile penetration into the target. The remaining yarns within the region up to which the longitudinal wave has reached along the radial direction are called secondary yarns. During the impact event, compression of the target takes place directly below the projectile. This region is referred as region 1. As a result of compression in region 1, the surrounding region would be under tension along the radial direction. This region is referred as region 2.

Generally, the impact event can be divided into three stages. During the first stage, the projectile strikes to the target, and compression of the target takes place directly below the projectile face. As the compression progresses, the material would flow predominantly along the thickness direction. Material flow can also be in the radial direction as well as toward the front face of the target. Material flow toward the front face of the target leads to the deformation along that direction. This is called as reverse bulge formation on the front face. This stage would continue until through-the-thickness compressive wave reaches to the back face of the target. During this stage, compressive stresses are generated within the target directly below the projectile. As a result of this, the surrounding region would be under tension along the radial direction.

Additionally, because of the impact force shear stresses are generated within the target around the periphery of the projectile. Any of these stresses could lead to failure of the target. As the projectile moves further, the yarns in region 2 of the upper layers exert pressure on the yarns in region 2 of the lower layers. In other words, compressive deformation of the yarns takes place also in region 2. Because of the compression of the layers, as well as possible failure of the target by different modes, the projectile moves further. This leads to bulge formation on the back face. This is the second stage of impact. Along with bulge formation on the back face, failure of the yarns/layers would take place by different mechanisms in the upper layers of the target. This process continues, and the projectile moves further. A clear plug formation can take place in front of the projectile. Also, the yarns/layers can fail in tension on the back face because of bulge formation.

During the third stage, the projectile moves further, and the plug and the projectile exit from the back face of the target. During the entire ballistic impact event, in-plane matrix cracking and delamination between the layers can also take place. As the projectile penetrates into the target and starts moving further, frictional forces act between the projectile and the target. Heat can also be gener-

ated during this process. Possible energy-absorbing mechanisms are discussed next.

A. Compression

When the specimen is impacted, initial compression takes place within the target directly below the projectile. As the induced stress exceeds the elastic limit, the specimen goes into plastic range. At this stage there can be higher compressive stress in the target directly below the projectile. Also, there can be tensile stress in the radial direction in the upper layers in region 2 and the shear stress along the thickness direction. During this stage, the failure can take place as a result of any of these mechanisms. Compression of the target continues until the compressive wave reaches to the back face of the target. The bulging process starts as soon as the compressive wave reaches to the back face of the target. During the compression stage, the material can fail in the form of matrix cracking. But the penetration of the projectile into the target is possible only after the yarns are broken either by shear plugging or as a result of in-plane tensile stress along the radial direction or as a result of the combined effect of both the mechanisms.

B. Reverse Bulge Formation on the Front Face

The reverse bulge formation can take place on the front face of the target. The effect is caused by the initial compression of the target and possible material flow toward the front face of the target. Delamination and matrix cracking contribute to bulge formation to some extent. This takes place during the first stage. Bulge formation also occurs as a result of the heat generated during the initial part of the impact.

C. Compression in the Surrounding Region of Impacted Zone: Region 2

During the impact event, compression of the target takes place directly below the projectile. This region is referred as region 1. As a result of compression in region 1, the surrounding region would be under tension along the radial direction. This region is referred to as region 2. Additionally, because of the impact force shear stresses are generated within the target around the periphery of the projectile. As the projectile moves further, the yarns in region 2 of the upper layers exert pressure on the yarns in region 2 of the lower layers. In other words, compressive deformation of the yarns in region 2 also takes place.

D. Yarns in Tension

Tensile failure of the yarns can take place on the front face as well as on the back face of the target. The tensile strain in the yarns varies with depth of the target and also with time. The tensile strain in the radial direction depends on the compressive wave propagation along through-the-thickness direction. Initially, the tensile strain in radial direction would be present only in the upper layers. As the compressive wave progresses toward the back face, the tensile strain in the radial direction would also be induced in the further layers. The tensile strain in the radial direction near the lower layers is essentially because of bulge formation on the back face. The bulge formation starts as soon as the compressive wave reaches to the bottom layer. Tensile failure would take place here as a result of stretching of the yarns. The strain in the bottom layer would now increase, and the layer would fail as the strain reaches to the limit. The failure of the yarns continues until the shear wave reaches to the back face or the complete failure of the target takes place. The strain in the yarns at the center would be more and would decrease gradually in the adjacent yarns. Even those yarns that do not fail in tension, but are in tension, can also absorb some energy.

E. Shear Plugging

Because of the contact force generated during the impact event, shear stresses are generated within the target around the periphery of the projectile. As the induced shear stress exceeds the permissible shear plugging strength, the yarns/layers would break. Also the layers can fail because of the radial tensile stress. The shear plug

can be formed as a result of shear plugging failure or tensile failure or as a result of the combined effect of both. High stresses are created at the point of impact. The material around the periphery of the projectile is sheared and pushed forward, causing a hole or "plug." Upon impact on the target, if the projectile energy is sufficient to cut the fibers by shear plugging, the first layer would fail because of shear plugging. This process would continue in the further layers until the kinetic energy of the projectile is more than the energy necessary to break the yarns either by shear plugging or breaking of yarns by induced tensile stress. Otherwise, the yarns are pushed forward, leading to bulge formation on the back face. The final failure would take place because of the induced tensile stress along the radial direction.

F. Bulge Formation on the Back Face

When the target is impacted transversely, compressive wave travels along the thickness direction. As soon as the wave reaches the back face of the target, the bulge formation starts. Bulging initiates the tensile failure of the fibers on the back face of the target. The strain varies along the thickness direction and also with time. The bulge formation continues until the material of the target fails either in tension or as a result of shear plugging or the combined effect of both. The bulge formation on the back face would stop if the velocity of the projectile reaches zero within the target.

G. Delamination and Matrix Cracking

During transverse impact event, compressive wave and shear wave propagate along the thickness direction. Also tensile and shear wave propagate along the radial direction within the layers. During this stage, as the induced stress exceeds the damage threshold stress, damage initiation would take place within that region. The damage can be in the form of delamination or matrix cracking. Delamination can also take place because of the bulging effect on the back face of the target.

H. Friction Between Projectile and Target and Heat Generation

During the ballistic impact event, the fiber/yarn breakage takes place because of shear plugging, tension in fibers/yarns, or because of the combined effect of both. As a result of this, a plug is formed in front of the projectile face. If the complete kinetic energy of the projectile is not absorbed by the target until the plug is formed, the projectile and the plug would move further toward the back face of the target. During this stage, there would be friction between the projectile and the target. This would absorb some kinetic energy of the projectile. In such cases when projectile has just enough kinetic energy to fracture all of the yarns but not enough kinetic energy to overcome the frictional resistance, the projectile can get stuck in the target. The extent of resistance offered by the target depends on the type of fit generated between the projectile and the damaged target. In other words, it depends on the surface condition of the hole formed within the target because of fiber/yarn breakage. When the projectile is moving within the target and the frictional resistance is offered, it can lead to local temperature rise. This would absorb some energy in the form of heat energy.

V. Analytical Formulation

As the projectile impacts onto the target, it loses some of its energy. This energy is absorbed by different energy-absorbing mechanisms of the target such as compression of the target directly below the projectile E_{cf} , reverse bulge formation on the front face of the target E_{rb} , compression of yarns/layers in the surrounding region of the impacted zone E_{csy} , tension in the yarns in the layer E_{tf} , shear plugging of the yarns E_{sp} , bulge formation on the back face of the target E_{bb} , delamination E_{dl} , matrix cracking E_{mc} , friction E_{fr} , and heat generated E_{hg} . Here, an analytical formulation is presented for the prediction of ballistic impact behavior of thick composites. The formulation is based on energy balance between the projectile and the target and the wave theory. The energy-absorbing mechanisms just mentioned are considered in the formulation. The main objective of the analytical formulation is to predict the ballistic limit,

contact duration, and damage shape and size. The input parameters required are the geometrical and mechanical characteristics of the target and projectile.

Stress waves are generated within the target when it is impacted by the projectile. Because of transverse impact, compressive wave and shear wave propagate along the thickness direction, and tensile and shear wave propagate along the radial direction. The projectile applies forces on the target. The forces acting are the compressive force, inertial force, and frictional force. These forces act at various stages of the impact event. The impact phenomenon can be divided into three stages. In the first stage, the compression of the target takes place directly below the projectile. During the first stage the failure can take place as a result of tensile strain exceeding the permissible limit or as a result of shear plugging. During this stage, the reverse bulging of the target on the front face can take place. The first stage ends when the compressive wave along through the thickness direction reaches to the back face of the target.

Then the second stage starts. In this stage, the shear plug formation and bulge formation at the back face of the target take place. The bulge formation can lead to tensile failure of the fibers on the back face. The second stage ends when the material completely fails. The failure might be caused by shear plugging or tensile failure or the combined effect of both. Then the third stage starts. During this stage, the plug forms, and the projectile starts moving forward toward the back face of the target. A typical situation would be when the plug has exited from the back face of the target and the front tip of the projectile has just reached to the back face of the target with zero velocity. The incident ballistic impact velocity that leads to such a case is defined as ballistic limit velocity. The energy is absorbed by friction between the plug/projectile and the target.

The total kinetic energy of the projectile lost during the ballistic impact event is equal to the total energy absorbed by the target until that time. It is given by the following relation:

$$E_{\text{TOTALi}} = E_{cfi} + E_{rbi} + E_{csyi} + E_{tfi} + E_{spi} + E_{bbi} + E_{dli} + E_{mci} + E_{fri} + E_{hgi} \quad (1)$$

The following assumptions are made in the analytical formulation:

- 1) Projectile impact is normal to the surface of the target.
- 2) The projectile is cylindrical with a flat end and perfectly rigid.
- 3) The compressive stress is experienced along the thickness direction only within those layers through which the compressive wave has traveled. Also, compressive strain is uniform within those layers.
- 4) The shear plugging stress is experienced along the thickness direction only within those layers through which the shear wave has traveled. Also, shear plugging stress is uniform within those layers.
- 5) The plug formed is freely moving forward without offering any resistance with the target except the frictional resistance.
- 6) The peak tensile strain within the yarns is at the periphery of the projectile. Hence, the tensile failure of the yarns would take place at the periphery of the projectile.
- 7) The velocity of the projectile remains constant during each time interval.

The analytical formulation for the three stages is presented next.

A. Stage 1

As the projectile is impacted onto the target, the through-the-thickness compressive and shear waves along the thickness direction and tensile and shear waves along the radial direction are generated in the target. At this stage, the forces acting on the projectile are inertial force and compressive force. The inertial force is not uniformly distributed over the nose surface but depends on the shape of the nose. The inertial force is calculated by equating the work done by the reaction of the inertial force on the target to the change in the kinetic energy of the displaced material.²⁷ From this the following relation is obtained:

$$F_i = \frac{1}{2} \rho K A V^2(z) \quad (2)$$

For the cylindrical projectile with a flat end, $K = 1$ (Ref. 27). The compressive force is distributed uniformly on the projectile

nose surface in the direction of motion. It is given by the following relation:

$$F_c = \sigma_{cz}(z)A \quad (3)$$

The total force acting on the projectile is given by

$$F = F_i + F_c \quad (4)$$

These forces are acting on the effective mass of the projectile. The effective mass of the projectile includes the material of the target displaced by the projectile moving with it. The effective mass of the projectile used in the equation is, therefore, $m_0 + \rho A z$. This is based on considering the projectile has moved by a distance z . The equation of motion for the penetration process is

$$\begin{aligned} \frac{d}{dt}(mV) &= F_i + F_c \\ \frac{d}{dt}(mV) &= V \frac{dm}{dt} + m \frac{dV}{dt} = \frac{1}{2} K \rho A V^2 + \sigma_{cz}(z)A \end{aligned} \quad (5)$$

The rate of change of effective mass of the projectile is

$$\frac{dm}{dt} = \rho A \frac{dz}{dt} = \rho A V, \quad \frac{dV}{dt} = \frac{dV}{dz} \frac{dz}{dt} = V \frac{dV}{dz} \quad (6)$$

Substituting Eq. (6) into Eq. (5), the following relation is obtained:

$$\rho A V^2 + (m_0 + \rho A z) V \frac{dV}{dz} = \frac{1}{2} K \rho A V^2 + \sigma_{cz} A \quad (7)$$

The preceding equation is solved by separation of variables to calculate the velocity,²⁷ and the expression of velocity is obtained as

$$V(z) = \left\{ \left[V_i^2 + \frac{\sigma_{cz}(z)}{\rho(1 + 0.5K)} \right] \times \left(\frac{m_0/\rho A}{m_0/\rho A + z} \right)^{2+K} - \frac{\sigma_{cz}(z)}{\rho(1 + 0.5K)} \right\}^{\frac{1}{2}} \quad (8)$$

The time required for the projectile to penetrate distance z is calculated by the following expression:

$$t = \int_0^z \frac{1}{V(z)} dz = \int_0^z \left\{ \left[V_i^2 + \frac{\sigma_{cz}(z)}{\rho(1 + 0.5K)} \right] \times \left(\frac{m_0/\rho A}{m_0/\rho A + z} \right)^{2+K} - \frac{\sigma_{cz}(z)}{\rho(1 + 0.5K)} \right\}^{-\frac{1}{2}} dz \quad (9)$$

The velocity calculated by this method is used only for the first time interval. After the calculation of the velocity, the energy absorbed by different energy-absorbing mechanisms during this time interval is calculated. Knowing the initial kinetic energy of the projectile and the energy absorbed during the first time interval, the velocity of the projectile for the next time interval is calculated. By knowing the velocity, various parameters such as displacement of projectile, strain, contact force, and energy absorbed by different mechanisms are calculated for the given time interval. This procedure continues until the compressive wave reaches to the back face of the target. The shear wave follows the compressive wave in through-the-thickness direction. The formulation for the calculation of the distance traveled by the compressive wave and the shear wave along the thickness direction is presented later. At this point it is necessary to check whether the material has failed in compression, tension, or shear. As the compressive wave passes along the thickness direction, the corresponding layers would fail if the induced compressive strain exceeds the permissible compressive strain. The compressive failure can be in the form of matrix cracking, and the fibers might not have broken. In such a case the penetration of the

projectile into the target would not take place. The penetration would take place either by shear plugging of the layers or by tensile failure of the yarns within the layer. Shear plugging would take place if the induced shear plugging stress exceeds the shear plugging strength. The tensile failure of the material is calculated layer by layer as the tensile strain in each layer at each time increment is different. The energy is absorbed as a result of any of these failure mechanisms. The detailed calculations of the energy absorbed as a result of different failure mechanisms are given in the next section. The first stage ends, and the second stage starts as soon as the compressive wave along through the thickness direction reaches to the back face of the target.

B. Stage 2

The second stage begins as the compressive wave reaches to the back face of the target. As the second stage starts, the shear plugging or tensile failure from the front face of the target continues. The bulge formation at the back face also starts. The bulge formation stops when the material fails either in tension or shear plugging or because of the combined effect of both. The energy is absorbed by these failure mechanisms. Based on the energy absorbed by different mechanisms, the velocity for the next time interval is calculated. The second stage ends when the complete material failure takes place either because of shear plugging or tension in the yarns or because of the combined effect of both. After this the third stage starts.

C. Stage 3

The target fails during the second stage, and the plug formation takes place. The plug forms, and the projectile moves toward the back face of the target during the third stage. The frictional resistance would be offered by the target for this movement. The length of the plug formed, if it is not broken into pieces, can be calculated as

$$h_p = n_{lfs} h_l \quad (10)$$

The force acting during this stage would be only the frictional force. The third stage ends when the tip of the projectile reaches to the back face of the target.

D. Wave Velocity

Stress waves are generated within the target when it is impacted by the projectile as a result of transverse impact. Compressive wave and shear wave propagate along the thickness direction. It is assumed that the mechanical properties of the material are the same for all of the layers along the thickness direction. The wave velocities along the thickness direction are given by

$$V_{zl} = \sqrt{\frac{1}{\rho} \frac{d\sigma_{cz}}{d\varepsilon_{cz}}} \quad (11)$$

$$V_{zl} = \sqrt{\frac{1}{\rho} \frac{d\tau}{d\gamma}} \quad (12)$$

For the elastic waves, E and G are used instead of the local slopes as given in Eqs. (11) and (12). The distance traveled by compressive wave and shear wave along the through-the-thickness direction at any instant of time is

$$z_l = V_{zl} t \quad (13)$$

$$z_t = V_{zl} t \quad (14)$$

The number of layers through which the compressive wave has traveled is

$$n_{lsc} = z_l / h_l \quad (15)$$

By knowing these quantities, the compressive strain details along the thickness direction at various time intervals, and also for different depth of projectile penetration, are calculated.

As the projectile is impacted onto the target, tensile and shear waves along the radial direction are also generated in the target. The wave velocities can be calculated using Eqs. (11) and (12). But, in this case, the material properties are with respect to radial direction.

E. Compressive Strain

The compressive strain along the thickness direction is induced in the target during the first stage. During the second stage, as the material also moves with the projectile, the compressive strain is not significant. The compressive strain is experienced along the thickness direction only within those layers through which through-the-thickness compressive wave has traveled. It is assumed that the compressive strain is uniform within these layers. The compressive strain in each layer at any instant of time is given by

$$\varepsilon_{cz} = z/z_l \quad (16)$$

F. Tensile Strain

As the projectile is impacted on the target, compression of the target takes place directly below the projectile (region 1). As a result of this, the surrounding region (region 2) would be under tension along the radial direction. In other words, the yarns in this region would be stretched. This behavior would be observed only in those layers that are compressed because of impact. The extent to which the yarns of different layers are stretched is different for different layers. The yarns of particular layers fail in tension when the induced tensile strain exceeds the permissible limit. The area under the tensile stress-strain curve of the yarns/layers is used for calculating the energy absorbed per unit volume as a result of tension in the yarns. The volume of the stressed yarn is equal to the cross-sectional area of the yarn and the distance through which the plastic wave has traveled in that particular yarn/layer along the radial direction.

The calculation of tensile strain in a particular yarn/layer is given next. The geometrical details are presented in Fig. 3:

$$\begin{aligned} z_{pl} &= z - j \Delta h_{lc}, & x_{tl} &= x_t \frac{(n_{lsc} - j)}{n_{lsc}} \\ x_{llc} &= \sqrt{x_{tl}^2 + z_{pl}^2}, & \varepsilon_{txl} &= \frac{x_{llc} - x_{tl}}{x_{tl} + d/2} \end{aligned} \quad (17)$$

where $j = 0, 1, 2, \dots, n_{lsc}$.

Here, $j = 0$ indicates upper surface of the first layer, and $j = 1$ indicates the lower surface of the first layer as well as the upper surface of the second layer. Also, for the first layer $z_l = z$. Further, $x_{tl} = ab$ for the second-layer top surface, and $x_{llc} = ac$ for the second-layer top surface. The expression for strain in Eq. (17) is obtained considering that the strain is uniform throughout the length of the strained yarn (Fig. 4). The work done in straining the yarn can be calculated considering the area under the stress-strain curve and the volume of the strained yarn. But the strain along the length of the yarn is not uniform because of the stress wave attenuation as the wave travels

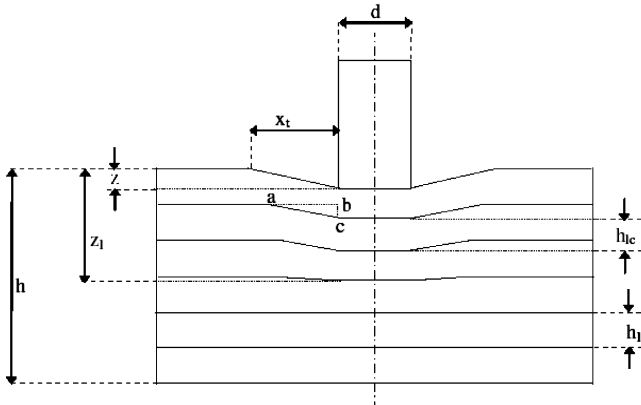


Fig. 3 Schematic arrangement showing tensile deformation behavior of woven fabric thick composite target during ballistic impact event.

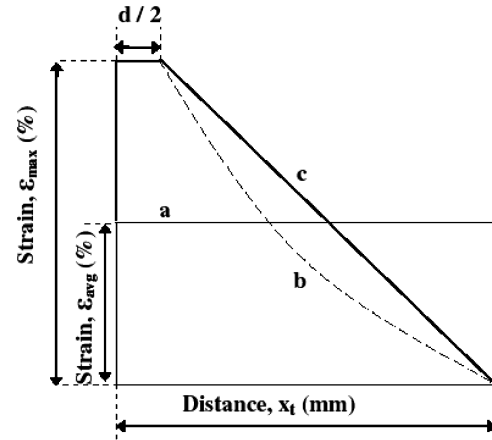


Fig. 4 Tensile strain variation in a yarn along the radial direction during ballistic impact event.

along the radial direction in a yarn. The stress would be maximum at the periphery of the projectile. It would be reducing gradually along the radial direction. Considering the work done for straining the yarns would remain the same, whether the strain is uniform along the length of the yarn or it is varying along the length of the yarn, the maximum strain at the periphery of the projectile can be calculated.

Considering the strain variation as linear with maximum strain at the periphery of the projectile and zero at a distance to which the longitudinal radial wave has reached at that particular time, the maximum strain is calculated as follows (Fig. 4):

$$\varepsilon_{txl}^{\max} = 2\varepsilon_{txl} \quad (18)$$

As the projectile moves forward during the ballistic impact event, it pushes the material ahead of it in a forward direction. As a result of this, the lower layers of the target would be pushed out even below the lower surface of the target. This phenomenon is bulging of the layers on the back face of the target. The layers present in these layers would be under tension. These layers can also fail under tension.

G. Deceleration History

In the beginning of the ballistic impact event, all of the energy is in the form of kinetic energy of the projectile. As the material fails, it absorbs some of the energy. The energy balance at the end of i th time interval is obtained as

$$\begin{aligned} KE_{p0} &= KE_{pi} + E_{cf(i-1)} + E_{rb(i-1)} + E_{bb(i-1)} + E_{tf(i-1)} + E_{sp(i-1)} \\ &+ E_{csy(i-1)} + E_{dl(i-1)} + E_{mc(i-1)} + E_{fr(i-1)} + E_{hg(i-1)} \end{aligned} \quad (19)$$

Rearranging the terms in the preceding equation,

$$\frac{1}{2}m_0V^2 - \sum_{i=1}^{i-1} E_{i-1} = \frac{1}{2}m_iV_i^2$$

or

$$\frac{1}{2}m_{i-1}V_{i-1}^2 - E_{i-1} = \frac{1}{2}m_iV_i^2 \quad (20)$$

Here

$$\begin{aligned} E_{(i-1)} &= E_{cf(i-1)} + E_{rb(i-1)} + E_{tf(i-1)} + E_{sp(i-1)} + E_{bb(i-1)} \\ &+ E_{csy(i-1)} + E_{dl(i-1)} + E_{mc(i-1)} + E_{fr(i-1)} + E_{hg(i-1)} \end{aligned} \quad (21)$$

The terms on the right-hand side of Eq. (21) can be calculated for each time interval. Hence, the velocity of the projectile for the next time interval is calculated as

$$V_i = \sqrt{\frac{\left(\frac{1}{2}m_{i-1}V_{i-1}^2 - E_{(i-1)}\right)}{\frac{1}{2}m_i}} \quad (22)$$

The deceleration of the projectile during i th time interval is obtained as

$$dc_i = \frac{V_{i-1} - V_i}{\Delta t} \quad (23)$$

The distance traveled by the projectile during i th time interval is obtained as

$$z_i = V_{i-1} \Delta t - \frac{1}{2} dc_i (\Delta t)^2 \quad (24)$$

The total distance traveled by the projectile is equal to the summation of the distance the projectile has traveled in each time interval. The force resisted by the target against the motion of the projectile is given by

$$F_i = m_i dc_i \quad (25)$$

This force is used to determine whether the shear plugging is taking place. The just-mentioned procedure is continued during all three stages of the ballistic impact event.

VI. Energy Absorbed by Different Mechanisms

A. Energy Absorbed as a Result of Compression of the Target

The target gets compressed along the thickness direction. Because of this, compressive strain is induced along the thickness direction. The total energy absorbed at that instant of time is given by

$$E_{cf} = A_p \left[\int_{\varepsilon_c=0}^{\varepsilon_{cz}} \sigma_{cz}(\varepsilon_{cz}) d\varepsilon \right] z_l \quad (26)$$

B. Energy Absorbed as a Result of Compression of Yarns in Region 2

As the projectile is impacted on the target, compression of the target takes place directly below the projectile (region 1). As a result of this, the surrounding region (region 2) would be under tension along the radial direction. Also the surrounding region would be under compression because of movement of the projectile along the through-the-thickness direction. Compression in the surrounding region absorbs some part of the initial kinetic energy of the projectile. The compression of the yarn is maximum at the periphery of the projectile and zero at a point up to which the transverse wave has traveled along the radial direction. A linear variation of compressive strain is assumed. The volume of the material that has been strained is obtained by the product of annular area between the projectile periphery and the distance up to which the transverse wave has traveled and the thickness of the layer. The energy absorbed is obtained as

$$E_{csy} = 2\pi h \sum_{j=nlf}^{n_{lsc}} \int_{d/2}^{x_l} \left[\int_{\varepsilon=0}^{\varepsilon=\varepsilon_{cz}} \sigma_{cz}(\varepsilon_{cz}) d\varepsilon \right] x dx \quad (27)$$

C. Energy Absorbed as a Result of Tension in Yarns

As the projectile is impacted on the target, compression of the target takes place directly below the projectile (region 1). As a result of this, the surrounding region (region 2) would be under tension along the radial direction. The calculation of tensile strain in a particular yarns/layer is given in Sec. V. The yarn at the center is strained the maximum. The yarn fails in tension if the induced tensile strain exceeds the failure strain. The total energy absorbed as a result of tensile failure of yarns is given by

$$E_{tf} = A_y \sum_{j=nlf}^{n_{lsc}} \int_0^{x_l} \left[\int_{\varepsilon=0}^{\varepsilon_{txl}} \sigma_{tx}(\varepsilon_{txl}) d\varepsilon \right] dx \quad (28)$$

The energy is absorbed by the yarns even before they fail. This is because of the elongation of the yarns. For such a case the energy absorbed as a result of yarns in tension would be based on strain at that time instant, not on the failure strain. The yarns would be under tension in the surrounding region, within the target, where the projectile has impacted. Also, the yarns can be in tension in the

lower layers because of bulging of yarns/layers on the back face of the target. The total energy absorbed as a result of tension is the sum of the energy absorbed by different yarns.

D. Energy Absorbed as a Result of Shear Plugging

At the point of impact, the compressive and shear waves are generated along the thickness direction. As the shear wave passes through a particular layer, if the shear stress exceeds the shear plugging strength shear plugging failure takes place. As a result of this, plug formation takes place. The energy absorbed by shear plugging during a time interval is given by the product of thickness of the target that is sheared, shear plugging strength, and the area over which shear stress is acting. It is given by

$$\Delta E_{spi} = n_s h_i S_{sp} \pi d h \quad (29)$$

The energy absorbed by shear plugging by the end of i th time interval is given by

$$E_{sp} = \sum_{n=1}^i \Delta E_{spi} \quad (30)$$

E. Energy Absorbed as a Result of Delamination and Matrix Cracking

Delamination and matrix cracking absorb some part of the initial kinetic energy of the projectile. The extent to which composite target has delaminated and the matrix has cracked until the i th time interval is calculated on the basis of strain profile along the radial direction in the composite target at that time interval (Appendix). The strain at the impact point is the highest, and it decreases along the radial direction from the point of impact. For the area in which the strain is more than the damage threshold strain, the target undergoes damage in the form of matrix cracking and delamination. However, complete matrix cracking does not take place. Evidence for this phenomenon is provided by the fact that after ballistic impact the matrix is still attached to the fibers and does not separate from the reinforcement completely. Because of matrix cracking, the interlaminar strength of the composite decreases. As a result, further loading and deformation cause delamination. This delamination is of mode II type. Again, delamination might not occur at all of the lamina interfaces. Towards the end of ballistic impact event, when only a few nondelaminated layers are left, these nondelaminated layers are more likely to bend rather than delaminate.

During the i th time interval, the energy absorbed by delamination and matrix cracking is given by

$$E_{dli} = P_d \pi x_d^2 A_{ql} G_{Ilcd}, \quad E_{mci} = P_m \pi x_d^2 A_{ql} E_{mt} h \quad (31)$$

During the ballistic impact event, the contact force is resisted mainly by the primary yarns; hence, the damage spread would be more along the primary yarns, that is, along the warp and fill directions compared with other directions. Hence the shape of the damage zone would be quasi-lemniscate and not circular. During the analysis, the damage spread along the primary yarns is calculated. Assuming the damage spread is the same along all of the directions, the damaged area would be circular. The quasi-lemniscate area prediction factor is introduced to take the area of actual shape. Quasi-lemniscate area reduction factor is defined as the ratio of area of quasi-lemniscate region and the corresponding circular area.

F. Energy Absorbed Due to Friction

As explained in Sec. IV, complete shear plugging/tensile failure of the target takes place during the second stage for the case of incident impact velocity equal to or greater than ballistic limit velocity, but the plug formed and the projectile are still within the target region. As the plug and the projectile start moving further during this stage, frictional resistance is offered by the target during the movement of the plug and the projectile. Generally, the plug formed is not in a solid form. Possibly, it is broken into pieces. Hence, in effect, the frictional resistance is offered only for the movement of the projectile.

Frictional resistance offered by the target toward the movement of the projectile is a material property. It depends on projectile diameter, length, and surface conditions. It also depends on the diameter of the hole formed within the target caused by ballistic impact, hole surface condition, and the target material properties. Frictional resistance is determined experimentally.

VII. Results, Validation, and Discussion

A. Experimental Studies

Typical experimental studies are conducted. The projectile and target information are given here:

1) The projectile is a cylindrical, flat-ended hardened steel projectile of diameter $d = 6.33$ mm, mass $m = 5.84$ g, and length $l = 24$ mm.

2) The target is a woven fabric E-glass/epoxy, unsupported area of the target 125×125 mm, thickness 4–7 mm.

The experimental ballistic limit velocity for the case of 5-mm thickness was 148 m/s, and for the case of 4-mm thickness was 137 m/s. When the experiment was carried out with the target thickness of 7 mm, complete penetration did not take place even with the incident ballistic impact velocity of 173 m/s.

Gellert et al.¹³ conducted ballistic impact experimental studies on woven fabric E-glass/vinylester composites with target thickness of 19, 14.5, and 9 mm using cylindrical, flat-ended steel projectiles. The experimental results are given in Table 1.

B. Input Data Necessary for the Analytical Predictions of Ballistic Impact Behavior

Ballistic impact behavior of typical woven fabric E-glass/epoxy composites has been studied. Mechanical properties of the target plate and the other details are given in Table 2 for a typical woven fabric composite studied. The same set of properties has been used for the study of materials used by Gellert et al.¹³ and Kumar and Bhat.¹¹

The compressive stress–strain curve along the thickness direction and tensile stress–strain curve along the radial direction for the woven fabric E-glass/epoxy composite at high strain rate are obtained by a separate study.

Details regarding load-displacement behavior under quasi-static loading for the study of frictional resistance are also obtained by a separate study. The plot obtained under quasi-static loading is used for the calculation of frictional energy during the ballistic impact event. The frictional resistance is offered by the target for the movement of the projectile during the third stage of the ballistic impact event. During this stage, the velocity of the projectile is less. Considering this, the plot obtained under quasi-static loading is used for the calculation of frictional energy during the ballistic impact event.

C. Comparison of Predicted and Experimental Results

Ballistic limit velocity has been predicted for different target thicknesses and projectile parameters using the analytical method and the mechanical and other properties presented in Table 2. The results are presented in Table 1 and compared with the experimental results. It can be seen that there is a good match between the analytically predicted and experimentally obtained ballistic limit velocities.

VIII. Ballistic Impact Behavior of Thick Composites

The energy absorbed by different energy-absorbing mechanisms, projectile kinetic energy, projectile velocity, contact force, distance traveled by the projectile, and longitudinal and shear waves along the thickness direction are evaluated as a function of time. Further, tensile strain at the failure of the layer is obtained as a function of time and target thickness. The distance up to which longitudinal and transverse waves have traveled along the radial direction until the failure of the layer and damage variation along the through-the-thickness direction are also presented. A typical case study is presented next.

The following data are used for generating Figs. 5–9:

- 1) The target material is a woven fabric E-glass/epoxy, where $h = 19$ mm.
- 2) The projectile parameters are $d = 6.35$ mm, $m = 3.84$ g, and $V = 550.894$ m/s.

Table 2 Input parameters required for the analytical predictions of ballistic impact behavior

Item	Reference	Data
Projectile (cylindrical)	Mass	5.84 g
	Shape	Flat ended
	Diameter	6.33 mm
	Material	E-glass/epoxy
	V_f	50%
	Thickness	5 mm
	No. of layers	19
	Density	1850 kg/m ³
	Tensile failure strain	3.5%
	Compressive failure strain	13.5%
Target	Shear plugging strength	90 MPa
	Compressive stress–strain curve	Plot
	Tensile stress–strain curve	Plot
	Quasi-lemniscate factor	0.9
	Delamination percentage	100%
	Matrix crack percentage	100%
	Strain energy release rate, mode II	1000 J/m ²
	Matrix cracking energy	0.9 MJ/m ³
Other	Frictional energy absorbed	Plot

Table 1 Ballistic impact test results and analytical predictions for typical woven fabric E-glass/epoxy composites

Projectile mass m , g	Projectile diameter d , mm	Target thickness h , mm	V_{BL} , m/s		Experiment results	Remarks
			Predicted	Experiment		
3.84	6.35, flat ended	19	550.894	563	Penetrated	Gellert et al. ¹³
3.84	6.35, flat ended	14.5	452.546	473	Penetrated	Gellert et al. ¹³
3.33	4.76, flat ended	19	508.80	505	Penetrated	Gellert et al. ¹³
3.33	4.76, flat ended	14	392.98	389	Penetrated	Gellert et al. ¹³
3.33	4.76, flat ended	9	269.03	293	Penetrated	Gellert et al. ¹³
5.84	6.33, flat ended	7	174.29	173	Not penetrated	Present study
5.84	6.33, flat ended	5	142.50	148	Penetrated	Present study
5.00	6.00, flat ended	25	559.112	547	Penetrated	Kumar and Bhat ¹¹

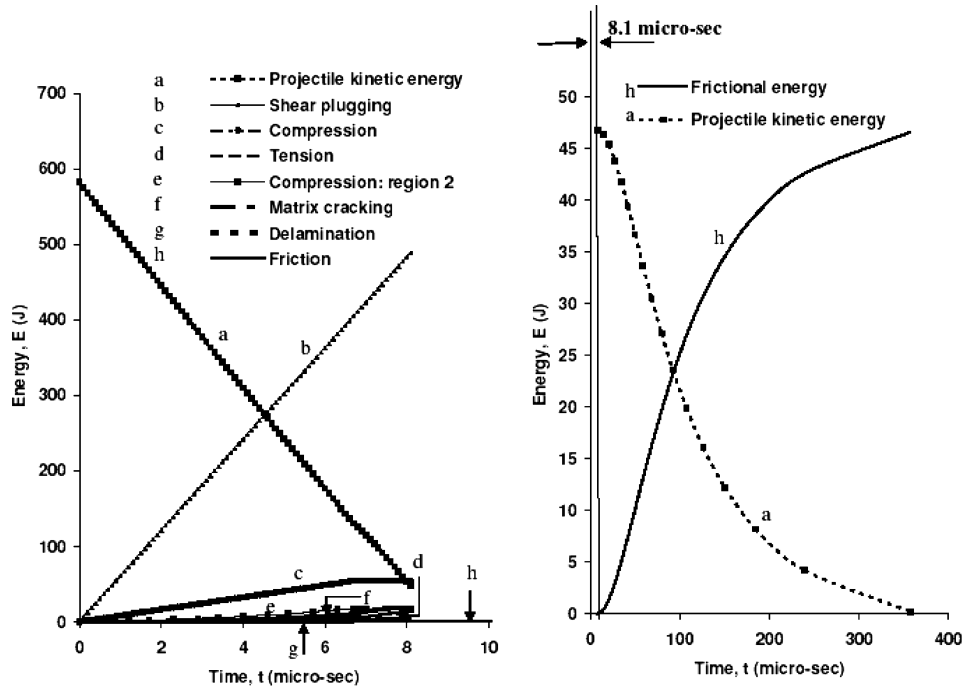


Fig. 5 Energy absorbed by different energy absorbing mechanisms during ballistic impact event: $V = 550.894 \text{ m/s}$, $m = 3.84 \text{ g}$, $d = 6.35 \text{ mm}$, $h = 19 \text{ mm}$, woven fabric E-glass/epoxy laminate.

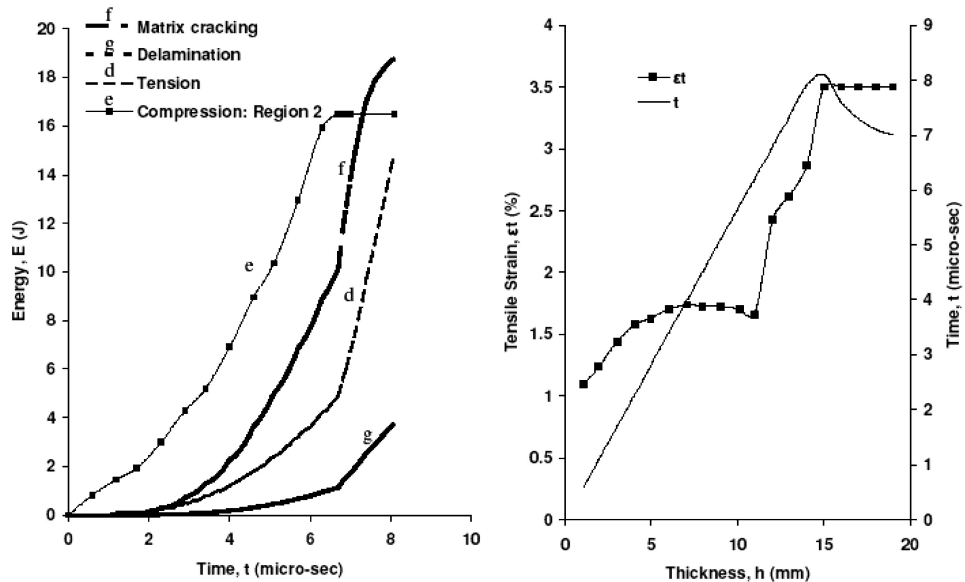


Fig. 6 Energy absorbed by different energy-absorbing mechanisms and tensile strain at failure of layer during ballistic impact event: $V = 550.894 \text{ m/s}$, $m = 3.84 \text{ g}$, $d = 6.35 \text{ mm}$, $h = 19 \text{ mm}$, woven fabric E-glass/epoxy laminate.

In this case, just the complete perforation of the target by the projectile took place, that is, the tip of the projectile was at the back face of the target at the end of the ballistic impact event. Hence, $V = 550.894 \text{ m/s}$ is the ballistic limit velocity. The projectile kinetic energy decreases during the ballistic impact event. This is because the energy is absorbed by the target by different mechanisms. As explained in Sec. IV, the ballistic impact event is subdivided into three stages. During the first two stages, damage is taking place up to the back face of the target, and the energy is absorbed by different mechanisms except for frictional energy. As can be seen from Fig. 5, for the case considered, the second stage ends at $8.1 \mu\text{s}$. During the third stage, energy is absorbed only because of the frictional resistance offered as a result of the movement of the projectile. For this case, at the end of the ballistic impact event, that is, at time

$359.43 \mu\text{s}$, the velocity of the projectile is zero (Fig. 7). The contact force increases during the first and second stages and decreases during the third stage.

The major energy-absorbing mechanism is shear plugging. Significant energy is absorbed by compression of target in the region directly below the projectile (region 1) and because of friction. Energy absorbed by matrix cracking, delamination, tension in the yarns, and compression in the surrounding region of the impacted zone (region 2) is relatively less (Fig. 6).

Tensile strain in the yarns at failure of different layers is shown in Fig. 6. It can be seen that the tensile strain exceeds the permissible tensile strain only in the last few layers. It indicates that only the last few layers fail in tension. The other layers fail because of shear plugging. Figure 6 presents the time interval when a particular layer

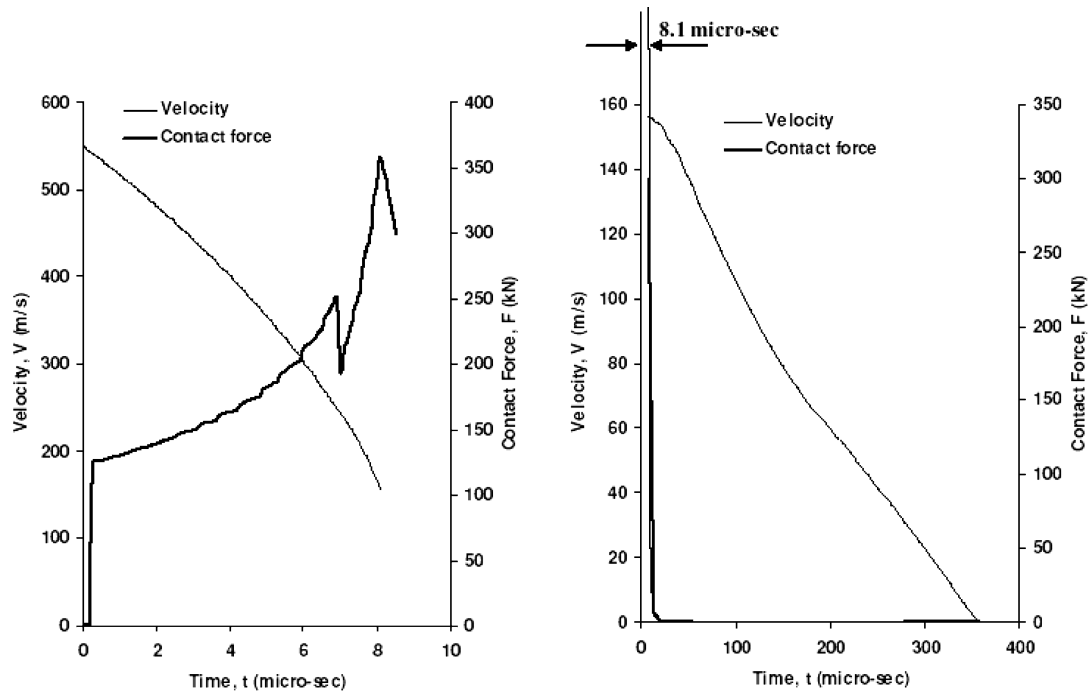


Fig. 7 Projectile velocity and contact force during ballistic impact event: $V = 550.894$ m/s, $m = 3.84$ g, $d = 6.35$ mm, $h = 19$ mm, woven fabric E-glass/epoxy laminate.

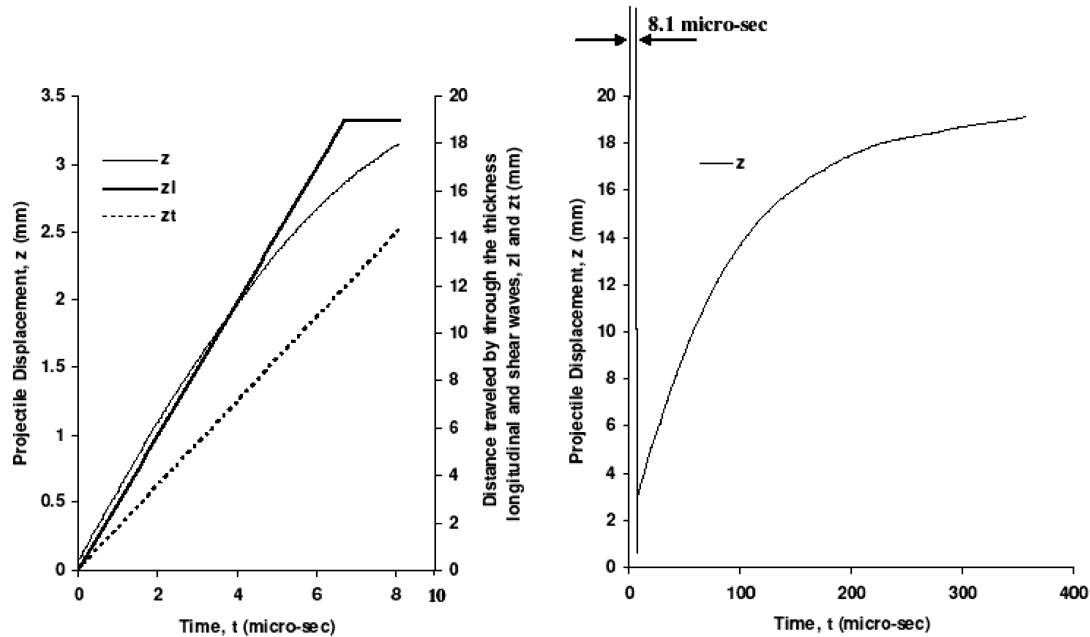


Fig. 8 Distance traveled by projectile and waves along the thickness direction during ballistic impact event: $V = 550.894$ m/s, $m = 3.84$ g, $d = 6.35$ mm, $h = 19$ mm, woven fabric E-glass/epoxy laminate.

fails, and it is plotted as a function of thickness. Among those layers that fail in tension, it can be seen that lower layers fail earlier than the layers above them. This is because of bulging effect on the back face of the target.

Projectile displacement during the ballistic impact event, that is, distance traveled by the projectile, is shown in Fig. 8. At the end of the second stage, the distance traveled by the projectile is 3.1 mm. At this stage all of the layers have failed either because of tension in the yarns/layers or because of shear plugging or because of the combined effect of both the mechanisms. After this, during the third stage the projectile along with the plug formed would move further toward the back face of the target. Because the velocity of the projec-

tile is less during this stage, the time taken for the projectile to move further is significantly higher. The distance traveled by through-the-thickness longitudinal and shear waves is also shown in Fig. 8. This would be only up to the end of second stage because the yarns/layers fail by the end of second stage.

Distance up to which transverse and longitudinal waves have traveled along the radial direction is shown in Fig. 9. The radial distance indicates the distance to which the waves have reached when the corresponding layers fail either because of tension or shear plugging or the combined effect of both the mechanisms. When the induced stress exceeds the permissible strength, the fracture of the yarns would take place. But much before that, clear damage zone

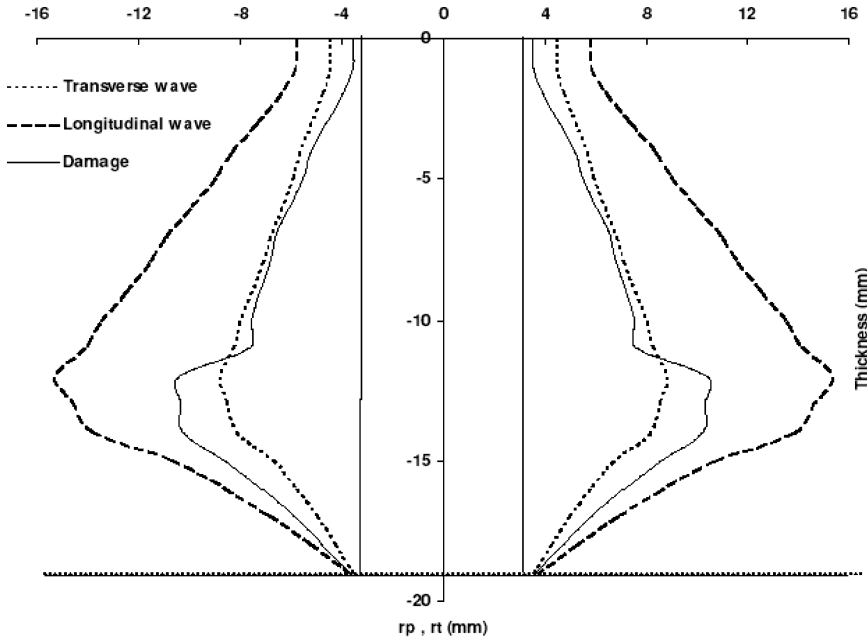


Fig. 9 Distance up to which transverse and longitudinal waves have traveled along the radial direction and damage variation along the thickness direction during ballistic impact event: $V = 550.894 \text{ m/s}$, $m = 3.84 \text{ g}$, $d = 6.35 \text{ mm}$, $h = 19 \text{ mm}$, woven fabric E-glass/epoxy laminate.

can be seen within the layers whenever the induced stress exceeds the damage initiation threshold stress. This damage is caused by either delamination or matrix cracking.

IX. Conclusions

An analytical method is presented for the prediction of ballistic impact behavior of thick composites. It is based on wave theory and energy balance between the projectile and the target. By using the analytical method, studies have been carried out on typical woven fabric composites.

The major energy-absorbing mechanism is shear plugging. Compression of the region directly below the projectile (region 1) and friction between the projectile and the target also absorb significant energy. Energy absorbed by matrix cracking, delamination, and tension in the yarns and compression in the surrounding region of the impacted zone (region 2) is not significant.

Appendix: Normalized Strain Profiles Along the Radius at Different Time Intervals

Figure A1 presents normalized strain profiles along the radius around the impacted zone at different time instants. This variation is because of stress attenuation. The maximum strain would be at the periphery of the projectile, and strain would decrease along the radius. Whenever the strain at the point of impact exceeds the permissible strain, the fiber/yarn breakage would take place because of tension. At that instant of time, sufficient damage would have occurred around the point of impact even though the strain is below the ultimate fiber/yarn fracture strain. If the strain in this region is above damage initiation threshold strain, clearly visible damage would be seen in this region. Normalized strain profiles at time t_a and t_b are shown in Fig. A1. At time t_a the damaged zone radius is d_a , whereas at time t_b the damaged zone radius is d_b . The radius d_b would nearly indicate the radius of damage zone at the end of ballistic impact event. The fiber fracture would take place at this time instant.

Damage initiation threshold stress can be explained with respect to tensile testing of composite specimens. As the specimen is loaded and it starts elongating, visible damage might not be seen. As the loading is increased, at certain stress level, clear damage can be seen in the form of matrix cracking and delamination. The stress level at which damage initiates is the damage initiation threshold stress. This is a material property. As the tensile load is further increased,

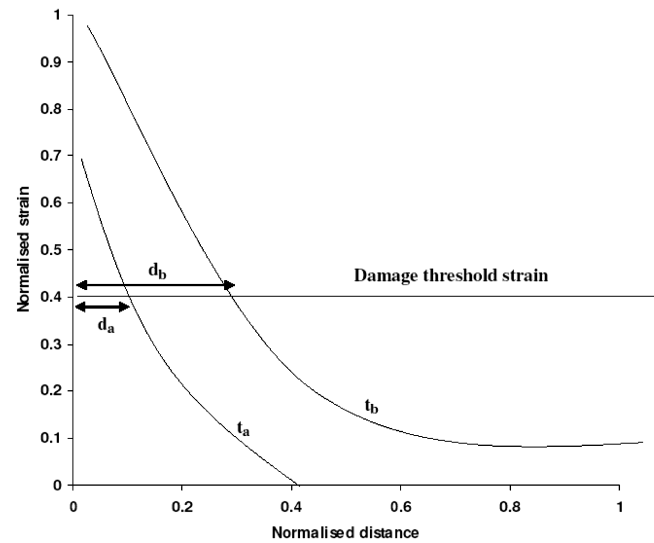


Fig. A1 Strain profiles at different time instants.

tensile fracture of the fibers/yarns would take place when the stress level reaches to the ultimate tensile strength value. Damage initiation threshold strain can be defined as a fraction of ultimate tensile strain value.

References

- ¹Zukas, J. A., "Penetration and Perforation of Solids," *Impact Dynamics*, edited by J. A. Zukas, T. Nicholas, H. F. Swift, L. B. Greszczuk, and D. R. Curran, Wiley, New York, 1982, pp. 155–183.
- ²Zhu, G., Goldsmith, W., and Dharan, C. H., "Penetration of Laminated Kevlar by Projectiles—I. Experimental Investigation," *International Journal of Solids and Structures*, Vol. 29, No. 4, 1992, pp. 339–420.
- ³Epstein, J. S., Deason, V. A., and Abdallah, M. G., "Impact Wave Propagation in Thick Composite Plate Using Dynamic Moiré Interferometry," *Optics and Lasers in Engineering*, Vol. 17, No. 1, 1992, pp. 35–46.
- ⁴Lee, S. W. R., and Sun, C. T., "Dynamic Penetration of Graphite/Epoxy Laminates Impacted by a Blunt-Ended Projectile," *Composites Science and Technology*, Vol. 49, No. 4, 1993, pp. 369–380.
- ⁵Zhou, G., and Davis, G. A. O., "Impact Response of Thick Glass Fiber Reinforced Polyester Laminates," *International Journal of Impact Engineering*, Vol. 16, No. 3, 1995, pp. 357–374.

⁶Wu, E., and Chang, L. C., "Woven Glass/Epoxy Laminates Subjected to Projectile Impact," *International Journal of Impact Engineering*, Vol. 16, No. 4, 1995, pp. 607–619.

⁷Iremonger, M. J., and Went, A. C., "Ballistic Impact on Fiber Composite Armors by Fragment Simulating Projectiles," *Composites Part A*, Vol. 27A, No. 7, 1996, pp. 575–581.

⁸Ellis, R. L., "Experimental Results, Ballistic Impact Resistance of Graphite Epoxy Composites with Shape Memory Alloy and Extended Chain Polyethylene Spectra Hybrid Components," M.S. Thesis, Mechanical Engineering, Virginia Polytechnic Inst. and State Univ., Blacksburg, VA, Dec. 1996, pp. 26–45.

⁹Potti, S. V., and Sun, C. T., "Prediction of Impact Induced Penetration and Delamination in Thick Composite Laminates," *International Journal of Impact Engineering*, Vol. 19, No. 1, 1997, pp. 31–48.

¹⁰Zee, R. H., and Hsieh, C. Y., "Energy Absorption Process in Fibrous Composites," *Materials Science and Engineering A*, Vol. 246, No. 1–2, 1998, pp. 161–168.

¹¹Kumar, K. S., and Bhat, T. B., "Response of Composite Laminates on Impact of High Velocity Projectiles," *Impact Response and Dynamic Failure of Composites and Laminate Materials, Part I, Key Engineering Materials*, Vol. 141–143, edited by J. K. Kim and T. X. Yu, Trans Tech Publications, Ltd., Brandrain, Uetikon-Zurich, Switzerland, 1998, pp. 337–348.

¹²Mines, R. A. W., Roach, A. M., and Jones, N., "High Velocity Perforation Behavior of Polymer Composite Laminates," *International Journal of Impact Engineering*, Vol. 22, No. 6, 1999, pp. 561–588.

¹³Gellert, E. P., Cimporeu, S. P., and Woodward, R. L., "A Study of Effect of Target Thickness on the Ballistic Perforation of Glass Fiber Reinforced Plastic Composites," *International Journal of Impact Engineering*, Vol. 24, No. 5, 2000, pp. 445–456.

¹⁴Rohchoon, P., and Jyongsik, J., "Effect of Laminate Thickness on Impact Behavior of Aramid Fiber/Vinylester Composites," *Polymer Testing*, Vol. 22, No. 8, 2003, pp. 939–946.

¹⁵Zhu, G., Goldsmith, W., and Dharan, C. H., "Penetration of Laminated Kevlar by Projectiles-II. Analytical Model," *International Journal of Solids and Structures*, Vol. 29, No. 4, 1992, pp. 421–436.

¹⁶Jenq, S. T., Jing, H. S., and Chung, C., "Predicting the Ballistic Limit for Plain Woven Glass/Epoxy Composite Laminate," *International Journal of Impact Engineering*, Vol. 15, No. 4, 1994, pp. 451–464.

¹⁷Potti, S. V., and Sun, C. T., "A Simple Model to Predict Penetration of Thick Composite Laminates Subjected to High Velocity Impact," *International Journal of Impact Engineering*, Vol. 18, No. 3, 1996, pp. 339–353.

¹⁸Gama, B., Bogetti, T. A., Fink, B. K., Mahfuz, H., and Gillespie, J. W., Jr., "Study of Through-Thickness Wave Propagation in Multi-Layer Hybrid Lightweight Armor," *Proceedings of the American Society for Composites, Thirteenth Technical Conference* [CD-ROM], edited by A. J. Vizzini, American Society for Composites, Los Angeles, 1998, pp. 1834–1848.

¹⁹Benloulo, C. I. S., and Sanchez-Galvez, V., "A New Analytical Model to Simulate Impact onto Ceramic Composite Armors," *International Journal of Impact Engineering*, Vol. 21, No. 6, 1998, pp. 461–471.

²⁰Wen, H. M., "Predicting the Penetration and Perforation of FRP Laminates Struck Normally by Projectiles with Different Nose Shapes," *Composite Structures*, Vol. 49, No. 3, 2000, pp. 321–329.

²¹Billon, H. H., and Robinson, D. J., "Models for the Ballistic Impact of Fabric Armor," *International Journal of Impact Engineering*, Vol. 25, No. 4, 2001, pp. 411–422.

²²Wen, H. M., "Penetration and Perforation of Thick FRP Laminates," *Composites Science and Technology*, Vol. 61, No. 8, 2001, pp. 1163–1172.

²³Phoenix, S. L., and Porwal, P. K., "A New Membrane Model for the Ballistic Impact Response," *International Journal of Solids and Structures*, Vol. 40, No. 24, 2003, pp. 6732–6765.

²⁴Naik, N. K., and Shrirao, P., "Composite Structures Under Ballistic Impact," *Composite Structures*, Vol. 66, No. 1–4, 2004, pp. 579–590.

²⁵Meyers, M. A., "Types of Elastic Waves," *Dynamic Behavior of Materials*, Wiley, New York, 1994, pp. 27–31.

²⁶Smith, J. C., McCrackin, F. L., and Schiefer, H. F., "Stress-Strain Relationships in Yarns Subjected to Rapid Loading—Part V: Wave Propagation in Long Textile Yarns Impacted Transversely," *Textile Research Journal*, April 1958, pp. 288–302.

²⁷Awerbuch, J., and Bodner, S. R., "Analysis of the Mechanics of Perforation of Projectiles in Metallic Plates," *International Journal of Solids and Structures*, Vol. 10, No. 6, 1974, pp. 671–684.

A. Palazotto
Associate Editor